

Stellar sources of dust in the high redshift Universe

Rosa Valiante^{1*}, Raffaella Schneider², Simone Bianchi² and Anja C. Andersen³

¹*Dipartimento di Astronomia, Università di Firenze, Largo Enrico Fermi 2, 50125 Firenze, Italy*

²*INAF - Osservatorio Astrofisico di Arcetri, Largo Enrico Fermi 5, 50125, Firenze, Italy*

³*Dark Cosmology Centre, Niels Bohr Institute, University of Copenhagen, Juliane Maries Vej 30, DK-2100 Copenhagen, Denmark*

Accepted . Received

ABSTRACT

With the aim of investigating whether stellar sources can account for the $\geq 10^8 M_\odot$ dust masses inferred from mm/sub-mm observations of samples of $5 < z < 6.4$ quasars, we develop a chemical evolution model which follows the evolution of metals and dust on the stellar characteristic lifetimes, taking into account dust destruction mechanisms. Using a grid of stellar dust yields as a function of the initial mass and metallicity over the range $1 - 40 M_\odot$ and $0 - 1 Z_\odot$, we show that the role of AGB stars in cosmic dust evolution at high redshift might have been over-looked. In particular, we find that (i) for a stellar population forming according to a present-day Larson initial mass function (IMF) with $m_{ch} = 0.35 M_\odot$, the characteristic timescale at which AGB stars dominate dust production ranges between 150 and 500 Myr, depending both on the assumed star formation history and on the initial stellar metallicity; (ii) this result is only moderately dependent on the adopted stellar lifetimes, but it is significantly affected by variations of the IMF: for a $m_{ch} = 5 M_\odot$, dust from AGB stars to dominate only on timescales larger than 1 Gyr and SNe are found to dominate dust evolution when $m_{ch} \geq 10 M_\odot$. We apply the chemical evolution model with dust to the host galaxy of the most distant quasar at $z = 6.4$, SDSS J1148+5251. Given the current uncertainties on the star formation history of the host galaxy, we have considered two models: (i) the star formation history obtained in a numerical simulation by Li et al. (2007) which predicts that a large stellar bulge is already formed at $z = 6.4$, and (ii) a constant star formation rate of $1000 M_\odot/\text{yr}$, as suggested by the observations if most of the FIR luminosity is due to young stars. The total mass of dust predicted at $z = 6.4$ by the first model is $2 \times 10^8 M_\odot$, within the range of values inferred by observations, with a substantial contribution ($\sim 80\%$) of AGB-dust. When a constant star formation rate is adopted, the contribution of AGB-dust decreases to $\sim 50\%$ but the total mass of dust formed is a factor 2 smaller. Both models predict a rapid enrichment of the ISM with metals and a relatively mild evolution of the carbon abundance, in agreement with observational constraints. This supports the idea that stellar sources can account for the dust observed but show that the contribution of AGB stars to dust production cannot be neglected, even at the most extreme redshifts currently accessible to observations.

Key words: Galaxies: evolution, high-redshift, ISM; quasars: general; stars: AGB and post-AGB, supernovae: general, ISM: dust, extinction

1 INTRODUCTION

It is estimated that 30% or more of the light emitted from stars in the Universe is absorbed and re-emitted by dust in the infrared (IR). The cosmic IR background, therefore, records the cumulative IR emission from galaxies at all redshifts and provides an important constraint on the global history of star formation. This emission is affected by dust evolution in galaxies, in particular at high redshift ($z > 5$), where the presence of dust can influence the galaxy number counts and the evolution of quasars (e.g. obscuring star-forming

galaxies or Active Galactic Nuclei; Smail, Ivison & Blain 1997; Hughes et al. 1998, Maiolino et al. 2003a).

Evidence for the presence of dust at high redshifts comes from observations of damped Ly α systems (Pettini et al. 1994; Prochaska & Wolfe 2002; Ledoux, Bergeron & Petitjean 2002) and from the detection of dust thermal emission from high redshift quasars (QSOs) selected from the Sloan Digital Sky Survey (SDSS) re-observed at millimetre wavelengths (Omont et al. 2001; Carilli et al. 2001; Bertoldi & Cox 2002). The inferred far-IR (FIR) luminosities of samples of $5 < z < 6.4$ quasars are consistent with thermal emission from warm dust ($T < 100$ K), with dust masses in excess of $10^8 M_\odot$ (Bertoldi et al. 2003; Robson et al. 2004; Beelen et al. 2006). Despite the fact that these high redshift quasars are rare

* E-mail: valiante@arcetri.astro.it

objects, hardly representative of the dominant star forming galaxy population, the FIR and sub-mm observations indicate that early star formation leads to rapid enrichment of their host galaxies Interstellar Medium (ISM) with metals and dust. This is consistent with the super-solar metallicities inferred from the optical emission-line ratios for many of these systems (Pentericci et al. 2002; Freudling et al. 2003; Maiolino et al. 2003b).

In present-day galaxies, the major sources of interstellar dust are believed to be low and intermediate-mass evolved stars during the Asymptotic Giant Branch (AGB) phase. Since these stars take a long time to evolve to their dust producing stages, it is commonly believed that they cannot be responsible for all of the dust seen at high redshifts. In fact, AGB stellar lifetimes (10^8 to 10^9 yr) are comparable to the age of Universe at redshift ≥ 6 (Morgan & Edmunds 2003; Marchenko 2006). As a result, if the observed dust is produced by stellar processes, supernova (SN) ejecta appear to be the only viable sites of grain condensation fast enough to explain these large dust masses.

This scenario has been tested through observations of the reddened quasar SDSSJ1048+46 at $z = 6.2$ (Maiolino et al. 2004) and of the Spectral Energy Distribution (SED) of the GRB 050904 afterglow (Stratta et al. 2007). In both sources, the inferred dust extinction curve is different with respect to any of the extinction curves observed at low z (Hopkins et al. 2004), and it shows a very good agreement with the extinction curve predicted for dust formed in SN ejecta. This is an indication that the properties of dust evolve beyond $z \sim 6$.

Theoretical models, based on classical nucleation theory, predict that a few hundred days after the explosions silicate and carbon grains can form in expanding SN ejecta, with condensation efficiencies in the range 0.1 – 0.3. This implies $\sim 0.1 - 1M_{\odot}$ of dust per SN for stellar progenitor masses in the range of core-collapse SN ($12 - 40M_{\odot}$) (Kozasa et al. 1991; Todini & Ferrara 2001; Clayton, Deneault & Meyer 2001; Nozawa et al. 2003).

There is now clear observational evidence for dust formation in core-collapse supernovae, but the quantity of dust formed within the ejecta is still a subject of debate. The observed IR emission for a limited number of SNe, such as 1987A (Wooden et al. 1993), 1999em (Elmhamdi et al. 2003) and 2003gd (Sugerman et al. 2006; Meikle et al. 2007) implies dust masses which are generally smaller than $10^{-3}M_{\odot}$, corresponding to condensation efficiencies which are at least two orders of magnitude smaller than what theory predicts. Observations of young galactic SN remnants by the *Spitzer* telescope provide unambiguous evidence of dust formation (Hines et al. 2004). The inferred total mass of freshly formed dust is $0.02 - 0.054M_{\odot}$ for Cas A (Rho et al. 2008), and $0.015M_{\odot}$ for 1E 0102.2-7219 (Rho et al. 2009). While masses up to $1 - 2M_{\odot}$ have been estimated from FIR and submm observations (Dunne et al. 2003), the interpretation of these data is complicated by strong foreground contamination (Krause et al. 2004; Wilson & Batrla 2005). The apparent discrepancies between observational estimates and theoretical models can be accommodated taking into account the partial destruction of newly synthesized dust in the reverse shock of the SN (Bianchi & Schneider 2007).

The evolution of dust in the early Universe is still poorly understood. Models developed so far show that the current observational constraints on dust production in SNe are still consistent with the scenario where most of the dust in QSO at $z \sim 6$ is produced by SNe. However these estimates either neglect dust destruction by interstellar shocks (Maiolino et al. 2006) or make extreme assumptions on SN dust condensation factors (Dwek, Galliano & Jones 2007).

It is clear that our ability to interpret the observed properties of high redshift QSOs depends on a detailed understanding of the star formation history and the history of metal and dust pollution in their host galaxies. This, in turn, requires an adequate description of metal and dust stellar yields.

In this work we study the evolution of dust produced by low, intermediate and high-mass stars as a function of time and metallicity, taking into account the stellar evolutionary timescales, i.e. without adopting an instantaneous recycling approximation. The aim of this study is to explore the relative importance of the two main stellar sources, AGB stars and SNe, in the evolution of dust at high redshift for galaxies with different star formation histories (SFH) and stellar Initial Mass Function (IMF).

The paper is organized as follows. In section 2, we describe the adopted grid of dust yields for AGB stars and SNe with different initial metallicities. In section 3 we discuss the time evolution of the predicted dust mass for two different SFH. In this section we also explore the dependence of the results on the adopted IMF and the stellar mass-lifetime relation. In section 4 we present a chemical evolution model which includes dust destruction by interstellar SN shocks and, in section 5, we apply it to the QSO SDSS J1148+5251 at $z = 6.4$, using the star formation history of the host galaxy predicted by the numerical simulation of Li et al. (2007). Finally, in section 6 we discuss and summarize the results of our work. In what follows, we assume a Λ CDM cosmology with $\Omega_m = 0.3$, $\Omega_{\Lambda} = 0.7$, $\Omega_b = 0.04$, and $H_0 = 70$ km/s/Mpc. The age of the Universe at a redshift $z = 6.4$ is about 840 Myr.

2 STELLAR SOURCES OF DUST

Dust production in the ISM is extremely inefficient as the timescales for dust formation are longer than the destruction timescales (Tielens 1998). Thus, formation sites during stellar evolution are required to explain the vast amounts of dust observed in the Universe.

Most of the theoretical models for dust formation are based on classical nucleation theory (Feder et al. 1966): the formation of solid materials from the gas phase can occur only from a vapour in a supersaturated state. Condensation of a given species occurs when its partial pressure in the gas exceeds its vapour pressure in condensed phase (Whittet 1992), with subsequent particle growth by random encounters leading to cluster formation. Chemical reactions will further assist cluster production. The rate of grain growth therefore depends on the temperature, T_g , and pressure, P_g , of the gas and the condensation temperature of a species, T_c . The optimum conditions for nucleation are thought to occur in the range $10^{-8} \leq P_g(\text{Pa}) \leq 10^5$ and $T_g \leq 1800$ K (Salpeter 1974). This gives very stringent restrictions on where nucleation can occur.

Stars seen to produce dust, only satisfy the conditions needed for the nucleation processes at the very latest stages of their evolution. The main stellar sites of dust grain condensation are the cool, dense atmospheres of AGB stars and the expanding SN ejecta. The type of dust formed depends on the relative abundance of carbon and oxygen at the onset of nucleation.

In this work, we use the results obtained by Bianchi & Schneider (2007) to estimate the mass and properties of dust formed in Type II SN ejecta and those presented by Zhukovska, Gail & Tieloff (2008) to take into account grain condensation in the atmospheres of AGB stars.

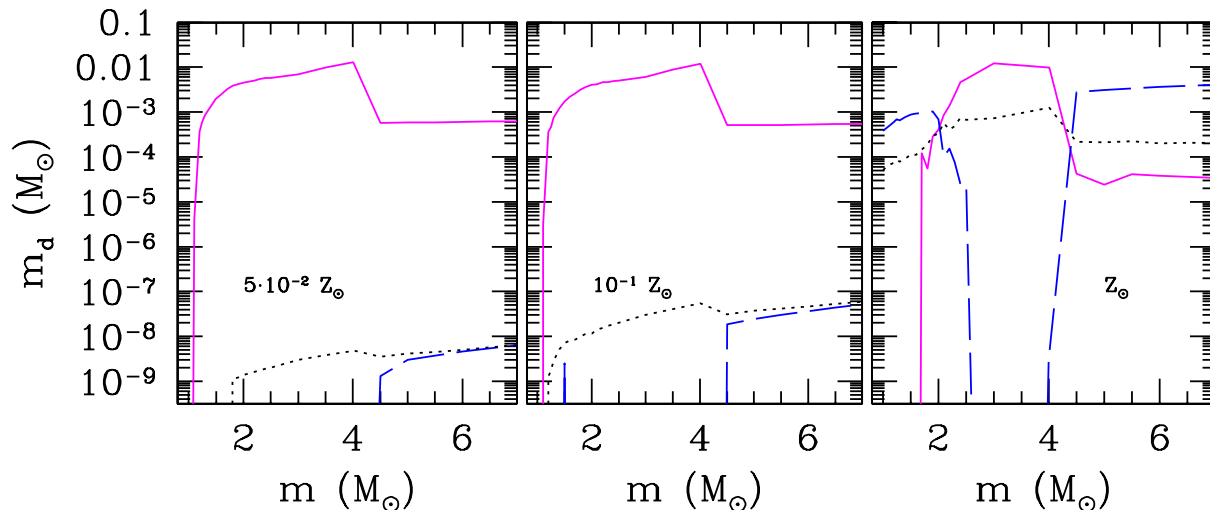


Figure 1. Dust masses returned by AGB stars as a function of the initial stellar mass for three different initial metallicities: $5 \times 10^{-2} Z_{\odot}$ (left panel), $10^{-1} Z_{\odot}$ (central panel) and Z_{\odot} (right panel). In each panel, the dust mass is separated into three main components: carbon (solid line), silicate (dashed line), and other dust (the latter component here represents the sum of Fe and SiC dust, dotted line). The results are taken from the grid of models by Zhukovska et al. (2008).

2.1 Dust produced by AGB stars

All stars with initial masses $0.8 M_{\odot} \lesssim m \lesssim 8 M_{\odot}$ on the main sequence evolve through the AGB phase of stellar evolution shortly before they become white dwarfs. In these stars, the sites of dust production are their cool, dense atmospheres during the thermally pulsating (TP) AGB phase. In this evolutionary stage, stars lose mass at an extremely high rate by a stellar wind and develop optically thick circumstellar dust shells by condensation of solid particulates in the outflowing gas.

Depending on the relative abundances of carbon and oxygen (C/O) of the ejected matter in which grains are formed, different dust mixtures are produced. Ferrarotti & Gail (2006) provide models which consistently describe the dependence of dust production by AGB stars on stellar initial mass and metallicity. They calculate the dust production rate of the dominant dust species, namely silicates, carbon, silicon carbide (SiC) and iron, which are formed from the most abundant elements. They use AGB stellar yields from van den Hoek & Groenewegen (1997) and Karakas et al. (2003).

On the basis of this model calculations, Zhukovska et al. (2008) propose refined grids of the ejected mass of different dust species, for different star masses in the range $(1 - 7) M_{\odot}$ and at various (sub-solar and solar) metallicities. These models predict that silicate dust is produced by stars with initial masses $< 1.5 M_{\odot}$ and $> 4 M_{\odot}$, which during the AGB phase are oxygen-rich. These stars are spectroscopically identified as M (characterized by $C/O < 1$) and S type ($C/O \approx 1$). On the other hand, carbon and SiC dust production is dominated by stars with initial mass $(1.5 - 4) M_{\odot}$, during the carbon-rich phase of evolution on the AGB (C stars, $C/O > 1$). Iron dust should be formed in all M, S and C type stars. However, only some hints of its existence have been found up to now (e.g. Kemper et al. 2002).

To ease the comparison with the dust mass produced by SNe, in Fig. 1 we plot the mass of carbon, silicate and *other* dust species produced by AGB stars as a function of the initial star mass and for three different metallicities, $(5 \times 10^{-2}, 10^{-1}, 1) Z_{\odot}$. Here we indicate as *other* dust the sum of iron and SiC grains. It is clear from the figure that AGB stars can produce $10^{-5} < M_{\text{carb}}/M_{\odot} \lesssim 10^{-2}$

at all metallicities while comparable amounts of silicate can only be produced when $Z \sim Z_{\odot}$. In fact, silicate grain condensation requires the presence of a sufficient amount of Si, O, Mg and Fe in the stellar outflow. These metal species cannot be produced by the star and have to be collected by the pre-enriched ISM prior to star formation.

2.2 Dust produced by SNe

Stars with masses $m > 8 M_{\odot}$ end their life exploding as core-collapse SNe. Main sites of dust formation are their expanding ejecta, a few hundred days after the explosions. Dust formed in stellar winds during the pre-supernova phase (i.e. by Red Supergiant stars or Wolf-Rayet stars) is almost entirely destroyed by the subsequent shock wave (see discussion in Zhukovska et al. 2008 and references therein).

Most of the available models proposed to investigate the process of dust formation in expanding SN ejecta are based on classical nucleation theory and grain growth. The onset of grain formation depends on the temperature structure in the SN ejecta, whereas the grain composition mainly reflects its chemical composition, which depends on the nucleosynthesis occurring during stellar lifetime (i.e. on the progenitor mass) and explosion mechanism. Thus, models of dust formation in SN ejecta are based on specific prescriptions for the chemical composition and thermodynamics of the expanding gas.

For the present analysis, we use the results of the model initially developed by Todini & Ferrara (2001) but recently revisited by Bianchi & Schneider (2007) in order to follow the evolution of newly condensed grains from the time of formation to their survival through the passage of the reverse shock in the SN remnant. In these works, the ejecta are taken to have a uniform composition and density, with initial temperature and density chosen to match the observations of SN1987A. The initial composition depends on the metallicity and mass of the progenitor star while the dynamic is given by the mass of the ejecta and the kinetic energy of the explosion: the initial SN models were taken from Woosley & Weaver (1995). Therefore, we consider dust formed in the ejected matter by SNe with initial progenitor star masses in the range $(12 - 40) M_{\odot}$ and

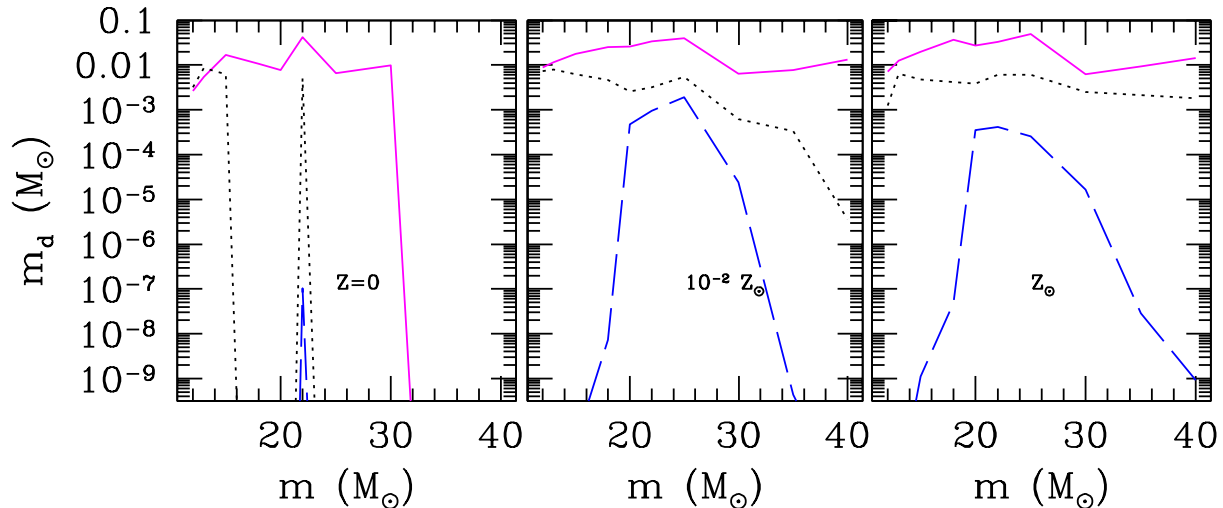


Figure 2. Dust mass returned by supernovae as a function of the stellar progenitor mass and for three different initial metallicities, 0 (left panel), $10^{-2}Z_{\odot}$ (central panel) and Z_{\odot} (right panel). These models refer to an assumed ISM density of $\rho_{\text{ISM}} = 10^{-24} \text{ g cm}^{-3}$, when 7% of the original dust mass survives the passage of the reverse shock. The three main dust species are compared: graphite (solid line), silicates (dashed line) and other species, which here represents the sum of Fe_3O_4 and Al_2O_3 grains (dotted line).

metallicities (0, 10^{-4} , 10^{-2} , 10^{-1} , 1) Z_{\odot} . Bianchi & Schneider (2007) derive the fraction of dust which survives the passage of the reverse shock, as a function of progenitor star mass and metallicity. Dust destruction due to the passage of the reverse shock depends on the density of the surrounding ISM. The denser is the gas in the ISM, the higher is the fraction of the destroyed dust mass. We refer the reader to the original paper for more details on the model.

In what follows, we adopt the results of the reference model by Bianchi & Schneider (2007), i.e. the model which starts grain condensations from seed clusters made of $N \geq 2$ monomers, assumes a sticking coefficient $\alpha = 1$ (all the gas particles colliding on a grain will stick to it) and an ISM density of $\rho_{\text{ISM}} = 10^{-24} \text{ g cm}^{-3}$. In this model, about $0.1 - 0.6 M_{\odot}$ of dust are formed in the ejecta but only 7% of the initial dust mass survives the passage of the reverse shock. Note, however, that these numbers are sensitive to variations on the assumed values of N , α and ρ_{ISM} . For a larger N and/or a smaller α , dust grains are characterized by smaller radii, which are more easily destroyed. If the SN explodes in a denser ($\rho_{\text{ISM}} > 10^{-23} \text{ g cm}^{-3}$) ISM, only about 2% of the dust mass survives. Conversely, for a lower density ISM ($\rho_{\text{ISM}} = 10^{-25} \text{ g cm}^{-3}$) a larger fraction, about 20%, is left.

In Fig. 2 we present the final mass of carbon, silicate and other dust species (essentially magnetite, Fe_3O_4 , and corundum, Al_2O_3) for the fiducial model, as a function of the initial stellar mass and metallicity, as given by Bianchi & Schneider (2007). Carbon dust condensation efficiency does not vary much with metallicity, with $10^{-3} \leq M_{\text{carb}}/M_{\odot} \leq 10^{-1}$, while silicates production appears to be inefficient at low metallicity. It is worth noting that the model by Bianchi & Schneider (2007) shows that SNe are expected to produce mainly carbon, magnetite and corundum grains. This is at odd with the models developed by Nozawa et al. (2003, 2007), in which the composition is dominated by silicate and iron grains. The differences are likely to be due to different initial SN models and their assumption of complete formation of SiO and CO molecules. While the first molecule is necessary to study the formation of Si-bearing grains, the second may be a sink for carbon atoms that otherwise would accrete on grains (Bianchi & Schneider 2007). In both models, though, a similar amount of dust is formed and survives the

reverse shock. A thorough comparison between different theoretical models is deferred to future studies.

Finally, it should be mentioned that in the present model we do not consider the possible contribution to dust production by pair-instability and type Ia SNe. The former class is predicted to be the end-product of the evolution of very massive Population III stars with masses in the range $140M_{\odot} \leq M \leq 260M_{\odot}$ and might provide an important source of dust at high redshift (Schneider, Ferrara & Salvaterra 2004; Nozawa et al. 2003). However, our aim here is to compare the relative contribution of the two main stellar sources of dust assuming a conventional stellar initial mass function with an upper mass cut-off of $100M_{\odot}$. For the latter class, there are no available theoretical models for dust production and destruction, although Clayton et al. (1997) have presented arguments in favor of dust production in type Ia SNe, with important consequences for the composition of iron dust in the interstellar medium (Dwek 1998). Type Ia SNe might be relevant for dust evolution at high redshift given the recent observational evidence for a "prompt" component exploding in a time scale of the order of 100 Myr after the stellar birth (Mannucci, Della Valle & Panagia 2006) and that a sizeable fraction of stars with masses in the range $3 - 8M_{\odot}$ is predicted to explode as type Ia SNe (Maoz 2008). However, adding the contribution of type Ia SNe to (iron) dust production is beyond the scope of the present analysis.

3 COSMIC DUST YIELDS

As a first step of the analysis, we compute the time evolution of the total dust mass produced, $M_d(t)$, considering the contribution of AGB stars and Type II SNe discussed above. The aim of this study is to investigate the relative importance of these two formation channels and the characteristic timescales at which one dominates over the other.

We take into account that stars of different masses evolve on

different timescales¹. Therefore, the time evolution of the total dust mass can be expressed as:

$$M_d(t) = \int_0^t dt' \int_{m_*}^{100M_\odot} m_d(m)\phi(m)\text{SFR}(t' - \tau_m)dm, \quad (1)$$

where m is the progenitor stellar mass, m_d is the dust mass produced by a star of mass m , $\phi(m)$ is the stellar Initial Mass Function (IMF), SFR is the star formation rate, and τ_m is the stellar lifetime of a star of mass m . The lower limit m_* is the minimum progenitor mass contributing to the dust production at a time t' , i.e. the mass corresponding to a stellar lifetime $\tau_m = t'$.

Note that we have no prescriptions for dust production by stars in the mass range $(8 - 11) M_\odot$, which evolve as AGB and finally explode as core-collapse SNe (II-P SNe, Smartt et al. 2009). Dust yields for stars in this mass range (and for different metallicity) are not yet available in the literature. Therefore we extrapolate from the dust mass produced by the largest available AGB model ($7 M_\odot$) and by the smallest SN progenitor ($12 M_\odot$) to account for metal and dust production in this mass range. However, the contribution to the total mass of dust from stars in this mass range is less than 5%.

To investigate the dependence on the star formation history, we make two extreme hypotheses: (i) a burst occurring at $t = 0$, where all stars are born at the same epoch, in an instantaneous episode of star formation; (ii) a constant SFR, where stars form continuously and at a constant rate for 10 Gyr.

It is clear that the relative contribution of AGB stars and SNe depends on the shape of the stellar IMF and on the adopted stellar lifetimes. In our reference model, we assume that stars form with masses in the range $(0.1 - 100) M_\odot$ according to a Larson IMF (Larson 1998), which follows a Salpeter-like power law at the upper end but flattens below a characteristic stellar mass:

$$\phi(m) \propto m^{-(\alpha+1)} e^{-m_{ch}/m}, \quad (2)$$

where $\alpha = 1.35$, $m_{ch} = 0.35M_\odot$ and we normalize the integral of $m\phi(m)$ in the mass range $(0.1 - 100) M_\odot$ to unity. The lifetimes of stars of different mass and metallicity are computed according to the following simple parametric form proposed by Raiteri et al. (1996),

$$\log(\tau_m) = a_0(Z) + a_1(Z) \log m + a_2(Z)(\log m)^2, \quad (3)$$

where τ_m is expressed in yr, m in solar units and the coefficients are:

$$a_0(Z) = 10.13 + 0.07547 \log Z - 0.008084(\log Z)^2, \quad (4)$$

$$a_1(Z) = -4.424 - 0.7939 \log Z - 0.1187(\log Z)^2, \quad (5)$$

$$a_2(Z) = 1.262 + 0.3385 \log Z + 0.05417(\log Z)^2.$$

Although this relation has been tested to reproduce the stellar evolutionary data in the metallicity range $3.5 \times 10^{-3} \leq Z/Z_\odot \leq 1.5$, we apply it also to stars with lower metallicities.

In Fig. 3 we show the time evolution of the dust mass normalized to the final mass of stars for a burst-like (right panels) and a constant star formation history (left panels) and assuming that all stars form at the same initial metallicity of $Z = 0$ (upper panels)² (upper panels) and $Z = Z_\odot$ (lower panels). The curves represent

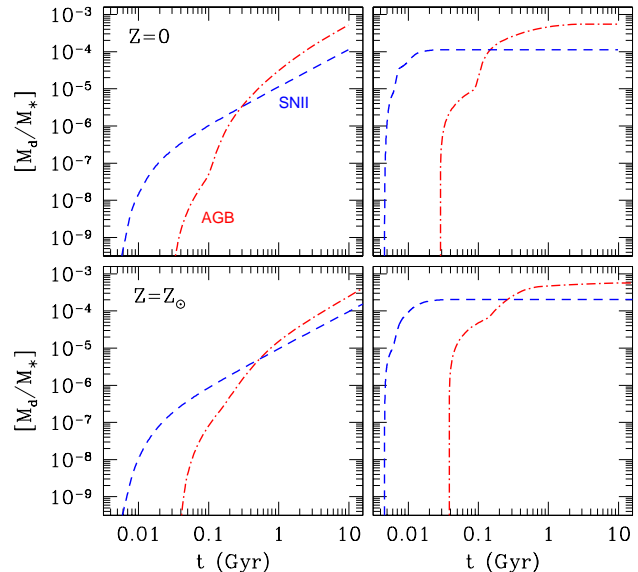


Figure 3. Time evolution of the mass of dust produced by SNe (dashed lines) and AGB stars (dot-dashed lines) normalized to the total mass of stars formed in 10 Gyr in our reference model (see text). All the stars have an initial metallicity of $Z = 0$ (upper panels) and $Z = Z_\odot$ (lower panels). The right panels show the results obtained assuming that star formation occurs in a burst at $t = 0$ whereas the left panels are computed for a constant star formation rate lasting for 10 Gyr.

the mass of dust, summed over all the components (carbon, silicates and other dust species) produced by SNe (dashed lines) and AGB stars (dot-dashed lines). At the beginning of the evolution, dust production is dominated by SNe; however, for $t > 30$ Myr the contribution of AGB stars rapidly increases and becomes dominant in a characteristic time which depends both on the assumed star formation history and stellar metallicity, ranging between 150 Myr (for a burst at $Z = 0$) and 500 Myr (for a constant star formation rate at $Z = Z_\odot$). These results suggest that AGB stars might give a non-negligible contribution to dust production at early cosmic epochs and that their role as dust factories at $z \geq 6$ might have been over-looked.

We have also investigated how these results depend on different model assumptions, such as the stellar lifetime relation and IMF. It can be shown that the timescales at which AGB stars start to be the dominant dust sources change by less than 20% if we adopt the stellar lifetimes proposed by Padovani & Matteucci (1993), which predicts slightly longer lifetimes for stars of intermediate mass and high metallicity compared to our reference model.

The largest uncertainty is introduced by the shape of the stellar IMF, which can be quantified through variations of the stellar characteristic mass m_{ch} in eq. 2. In Fig. 4 we show the time evolution of dust mass produced by SNe and AGB stars assuming a constant stellar metallicity of $Z = Z_\odot$ and three different values for the characteristic mass $m_{ch} = 1, 5, \text{ and } 10M_\odot$ (from bottom to top). As in Fig. 3, stars are formed at a constant rate for 10 Gyr (left

the same as at $Z = 5 \times 10^{-2} Z_\odot$. For both AGB and SN dust, dust mass values at metallicities not available in the grids are obtained through interpolation.

¹ The characteristic times for dust formation in AGB and dust formation/evolution in SNe are negligible compared to the star lifetime (Bianchi & Schneider 2007).

² As the grids of Zhukovska et al. (2008) are not computed for $Z < 5 \times 10^{-2} Z_\odot$, we have assumed that the AGB dust mass for lower metallicities is

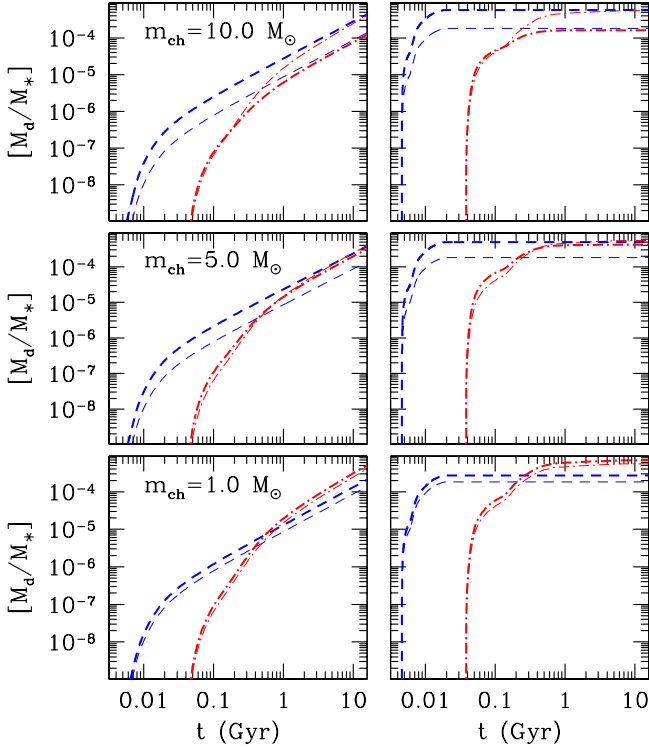


Figure 4. The same as in Fig.3 but assuming that all stars form with a metallicity $Z = Z_{\odot}$ and a Larson IMF with characteristic masses 1, 5, and $10M_{\odot}$ (from bottom to top); left panels are computed assuming a constant star formation rate for 10 Gyr; in right panels all stars are formed in a burst at $t = 0$. The mass of dust is normalized to the final stellar mass formed. For comparison, in each panel we also show the results of the fiducial model of Fig. 3 with thin lines.

panels) and in a burst at $t = 0$ (right panels) and the resulting dust mass is normalized to the total stellar mass formed. For comparison, in Fig. 4 the corresponding reference models are also shown (light curves).

As it can be inferred from the figure, the evolution is almost identical to the reference model for $m_{ch} = 1M_{\odot}$; for $m_{ch} = 5M_{\odot}$, the mass of dust contributed by SNe is increased (as a consequence of the larger SNe rate) and AGB stars produce a comparable amount of dust on timescales ~ 1 Gyr. Finally, when $m_{ch} = 10M_{\odot}$ the AGB dust component is always sub-dominant, as a result of the larger SN rate and of the smaller number of stars formed with intermediate masses. Thus, it is clear that variations of the stellar characteristic mass over cosmic history due to the smaller gas metallicity and/or to the larger cosmic microwave background temperature (see, e.g., Omukai et al. 2005) might significantly affect the origin and properties of dust in the high redshift Universe.

4 CHEMICAL EVOLUTION MODEL WITH DUST

In this section, we describe a simple chemical evolution model with dust which allows to follow the time evolution of the mass of gas, stars, metals in specific environments, such as high redshift galaxies and quasars, given the appropriate star formation history. We then apply this model to a “template” QSO host galaxy at high redshift.

In this model, we make the simplifying assumptions that (i) there are no mass exchanges with the surrounding intergalactic medium (IGM) (“close-box” model), and that (ii) dust produced

by AGB stars and SNe does not grow in molecular clouds (MC) by accretion of metals. Indeed, dust grains formed in stellar outflows can serve as growth centers for accretion of icy mantels in dense MC (e.g. Draine 1990). However, grain mantles are amorphous and heterogeneous, thus MC-grown dust has different properties from dust produced by stars and must be treated as a separate component (see e.g. Zhukovska et al. 2008 and references therein). Since we are primarily interested in the study of the relative contribution of the two main stellar sources, we do not follow the evolution of this component.

The model consists of a set of differential equations regulating the time evolution of the different components:

$$\frac{dM_*(t)}{dt} = \text{SFR}(t) - \frac{dR(t)}{dt} \quad (6)$$

$$\frac{dM_{\text{ISM}}(t)}{dt} = -\text{SFR}(t) + \frac{dR(t)}{dt} \quad (7)$$

$$\frac{dM_Z(t)}{dt} = -Z_{\text{ISM}}(t)\text{SFR}(t) + \frac{dY_Z(t)}{dt} \quad (8)$$

$$\frac{dM_d(t)}{dt} = -Z_d(t)\text{SFR}(t) + \frac{dY_d(t)}{dt} - \frac{M_d(t)}{\tau_d} \quad (9)$$

where M_* and M_d are the total masses of stars and dust, SFR is the star formation rate. Since a fraction of dust can be destroyed by interstellar SN shocks and returns metals back into the gas phase, we avoid complications indicating with M_{ISM} the total mass in the interstellar medium (gas and dust) and with M_Z the total mass of metals (diffused in the gas phase and condensed into dust grains). At any given time, the mass of *gas* can be computed as the difference between M_{ISM} and M_d , and the mass of *gas phase* metals as the difference between M_Z and M_d (with proper stoichiometric coefficients when we are interested in a particular gas phase element). The quantities $Z_{\text{ISM}}(t) = M_Z(t)/M_{\text{ISM}}(t)$ and $Z_d(t) = M_d(t)/M_{\text{ISM}}(t)$ are the total metal and dust abundances in the ISM. The terms dR/dt , dY_Z/dt and dY_d/dt represent the rates at which mass (gas and dust), heavy elements (gas-phase and condensed) and dust are returned to the ISM. These terms are given by:

$$\frac{dR(t)}{dt} = \int_{m_*(t)}^{100M_{\odot}} (m - \omega_m(m, Z_{\text{ISM}}))\phi(m)\text{SFR}(t - \tau_m)dm \quad (10)$$

$$\frac{dY_Z(t)}{dt} = \int_{m_*(t)}^{100M_{\odot}} m_Z(m, Z_{\text{ISM}})\phi(m)\text{SFR}(t - \tau_m)dm \quad (11)$$

$$\frac{dY_d(t)}{dt} = \int_{m_*(t)}^{100M_{\odot}} m_d(m, Z_{\text{ISM}})\phi(m)\text{SFR}(t - \tau_m)dm \quad (12)$$

where m is the initial mass of the progenitor star, and the lower limit m_* is the mass with a lifetime $\tau_m = t$. The total mass of metals (pre-existing and newly synthesized) produced by a star of initial mass m and metallicity Z , $m_Z(m, Z)$, and the mass of the stellar remnant $\omega_m(m, Z)$, are taken from van den Hoeck & Groenewegen (1997) for AGB stars with initial metallicities $Z = (5 \times 10^{-2}, 0.2, 1)Z_{\odot}$ and masses $1 - 8M_{\odot}$ and from Woosley & Weaver (1995) for SNe with initial masses $12 - 40M_{\odot}$ metallicities $Z = (0, 10^{-4}, 10^{-2}, 10^{-1}, 1)Z_{\odot}$. The grid of dust masses, $m_d(m, Z)$, is the same as described in section 2 and shown in Figs. 1 and 2. Note that integrating eq. 12 over time we obtain the mass of dust as given in eq. 1. The last term of eq. 9 is the dust destruction rate in the ISM by thermal sputtering in high-velocity ($v > 150 \text{ km s}^{-1}$) SN shocks. The destructive effect of the SN shock waves on dust grains depends on the dust species and on the destruction timescale, τ_d , i.e. the lifetime of the dust grains against destruction by SN remnant (Jones, Tielens & Hollenbach 1996). Following Dwek, Galliano & Jones (2007) we assume that

$$\tau_d = \frac{M_g(t)}{m_{\text{ISM}} R_{\text{SN}}}, \quad (13)$$

where m_{ISM} is the effective ISM mass that is completely cleared of dust by a single SN remnant (i.e. a measure of the grain destruction efficiency), which depends on the dust species, and R_{SN} is the SN rate,

$$R_{\text{SN}}(t) = \int_{m>8M_{\odot}}^{40M_{\odot}} \phi(m) \text{SFR}(t - \tau_m) dm. \quad (14)$$

Grain destruction efficiencies by radiative shocks have been modeled by Jones et al. (1994), and typical grain lifetimes of 0.6 and 0.4 Gyr have been estimated, respectively, for carbonaceous and silicate grains in the Milky Way (Jones et al. 1996). Dwek, Galliano & Jones (2007) investigate the dependence of grain destruction efficiency, m_{ISM} , on the ISM density, both for silicate and carbon dust. Following their study, for a uniform ISM with density $\rho_{\text{ISM}} = 10^{-24} \text{ g cm}^{-3}$, we assume $m_{\text{ISM}} = 1200 M_{\odot}$ for silicates and $800 M_{\odot}$ for carbon and other dust species. Finally, in what follows we always consider our fiducial model, i.e. a Larson IMF with a characteristic mass of $0.35 M_{\odot}$ and stellar lifetimes from Raiteri et al. (1996) as described in section 3.

5 THE MOST EXTREME QSO AT REDSHIFT 6.4

We apply the model described above to the most distant quasar, SDSS J1148+5251, discovered at redshift $z \approx 6.4$ (Fan et al. 2003). It is a very luminous quasar powered by a super massive black hole (SMBH) with mass $(1 - 5) \times 10^9 M_{\odot}$ accreting close to its Eddington limit (Willott et al. 2003). The FIR luminosity is $L_{\text{FIR}} \sim 10^{13} L_{\odot}$, suggesting a mass of dust in excess of $10^8 M_{\odot}$ (Bertoldi et al. 2003; Robson et al. 2004; Carilli et al. 2004; Beelen et al. 2006). If all the FIR emission is assumed to come from young stars, the derived SFR is about $3 \times 10^3 M_{\odot} \text{ yr}^{-1}$ (Bertoldi et al. 2003). Such a high SFR is also supported by the first detection of the carbon [CII] line at $158 \mu\text{m}$ (Maiolino et al. 2005). Alternatively, if the active galactic nucleus (AGN) contributes to dust heating, the inferred SFR would be much lower, in agreement with what implied by a simple application of the Schmidt-Kennicutt law adopting a total gas mass of $\sim 10^{10} M_{\odot}$ (Walter et al. 2004), which yields a value of $200 M_{\odot} \text{ yr}^{-1}$ (Dwek, Galliano & Jones 2007; Li et al. 2008).

The interpretation of the observed properties of J1148+5251 and of its host galaxy is therefore contradictory. Our aim here is to explore the relative importance of SNe and AGB in the build-up of the dust mass inferred for this system. We adopt the star formation history of the host galaxy of J1148+5251 predicted by a recent numerical simulation by Li et al. (2007). We then apply our chemical evolution model with dust and discuss the dependence of the results on the adopted star formation history. Note that this approach is not entirely self-consistent given that, as we will see below, the simulated system is not a closed-box. A more accurate study of the chemical properties of the host galaxy of J1148+5251 implementing dust evolution in the semi-analytical merger-tree code GAMETE (Salvadori, Ferrara & Schneider 2008) is currently underway.

The numerical simulation by Li et al. (2007) follows the hierarchical assembly of the SDSS J1148+5251 halo in a Λ CDM cosmology. Their model accounts for the quasar activity, the host galaxy properties and includes a self-regulated growth of the SMBH. The quasar host galaxy is found to form through seven major mergers of gas rich starburst progenitors between $z = 14.4$ and 6.4 . Intense starbursts are triggered by the gravitational interactions

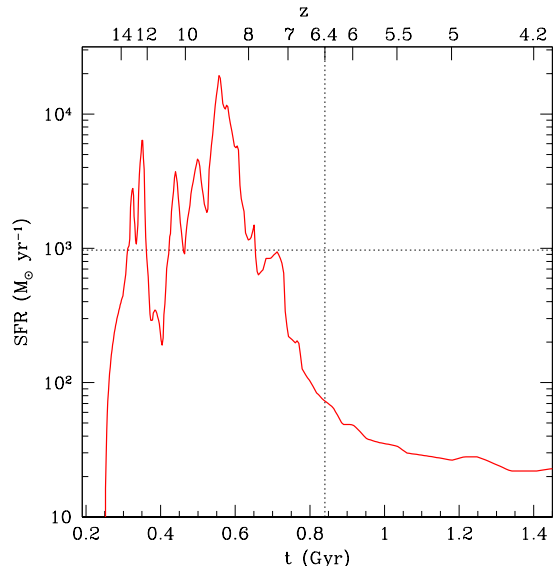


Figure 5. Time evolution of the star formation rate in the host galaxy of SDSS J1148+5251 as predicted by the simulation of Li et al. (2007). The rapid bursts of star formation are determined by strong successive interactions between the progenitor galaxies during a period of time ranging from about 0.29 Gyr (the time at which structure formation is set to begin) and 0.84 Gyr (the Hubble time at the quasar redshift $z = 6.4$). The SFR is expressed in $M_{\odot} \text{ yr}^{-1}$ and the time in Gyr. The horizontal line shows the average value of the star formation rate over the lifetime of the simulated QSO host galaxy, found to be $\sim 1000 M_{\odot} \text{ yr}^{-1}$, while the vertical line indicates the age of Universe (840 Myr) corresponding to a redshift $z = 6.4$, at which the quasar is observed.

between the merging galaxies and rapid black hole accretion is fuelled by the highly concentrated gas (see Li et al. 2007 for details). This model is able to reproduce most of the observed properties of SDSS J1148+5251, such as the black hole mass, the quasar luminosity and metallicity. For convenience, Fig. 5 shows the time evolution of the star formation rate found by Li et al. (2007). The star formation rate ranges between $\sim 100 M_{\odot} \text{ yr}^{-1}$, both at the onset of the interactions between the progenitor galaxies (at about 0.29 Gyr, corresponding to a redshift $z \sim 14$) and at the time of the final coalescence (0.8 Gyr, corresponding to $z \sim 6.5$), to values as large as $\sim 2 \times 10^4 M_{\odot} \text{ yr}^{-1}$ at the final major merger, represented by the peak at 0.6 Gyr ($z \sim 8.5$). The horizontal line shows the average value of the star formation rate over the lifetime of the simulated QSO host galaxy, found to be $\sim 1000 M_{\odot} \text{ yr}^{-1}$. Note that the simulation predicts a rate of about $100 M_{\odot} \text{ yr}^{-1}$ at 840 Myr (corresponding to redshift $z = 6.4$), an order of magnitude smaller than that inferred by FIR observations. Therefore, Li et al. (2008) suggests that the FIR luminosity of the QSO is not dominated by young stars but instead by the AGN (for over 80%). Finally, the stellar mass of the quasar host at $z = 6.5$ is predicted to be $\sim 10^{12} M_{\odot}$, in agreement with what would be required by the observed SMBH mass if the local black-hole-bulge relation were to hold at these high-redshifts. However, this result cannot be reconciled with observations of molecular gas: while the dynamical mass estimated from CO observations within 2.5 kpc from the QSO center is $\sim 5 \times 10^{10} M_{\odot}$, a conservative estimate of the contribution of the predicted stellar bulge within this region is a few $\times 10^{11} M_{\odot}$, about an order of magnitude larger (Walter et al. 2004).

Using the simulated star formation rate evolution as an input to

the chemical evolution model presented above, we can compute the corresponding evolution of the mass of stars and dust. Following Li et al. (2007), we assume that the QSO is hosted by a dark matter halo of mass $10^{13} M_{\odot}$ and that the initial mass in baryons is equal to the universal value, Ω_b/Ω_m , i.e. $\sim 1.3 \times 10^{12} M_{\odot}$.

In the left panel of Fig. 6 we show the evolution of the mass of stars (dotted line), and dust (solid line) of the host galaxy. The vertical solid lines indicate the age of Universe at $z = 6.4$ when the quasar is observed (840 Myr) and the data point represents the dust mass inferred from mm/submm observations by Beelen et al. (2006), $M_{\text{dust}} = 4.2 \times 10^8 M_{\odot}$, with error-bars which account for the range of values quoted in the literature, $(2 - 7) \times 10^8 M_{\odot}$. The lower dashed, dotted and dashed-dotted lines indicate the time evolution of the three main dust components, carbon, silicate and other dust grains, respectively. For these components, thin lines represent the contribution of AGB stars only.

The right panel shows the same quantities computed assuming a constant star formation rate equal to $1000 M_{\odot} \text{yr}^{-1}$ (the average value shown with the horizontal line in Fig. 5). In this model the total mass of stars formed at $z = 6.4$ is $\sim 4.3 \times 10^{11} M_{\odot}$, marginally consistent with the observed dynamical mass after correcting for the extension of the stellar bulge.

It is clear from the figure that our chemical evolution model with the simulated SFR predicts a total mass of dust of $M_{\text{dust}} = 2 \times 10^8 M_{\odot}$ at $z = 6.4$ in agreement with observations. We stress that this result is obtained following dust production by stellar sources on their characteristic stellar lifetimes and dust destruction by astration and SN shocks. The latter mechanisms are responsible for the down-turns in the evolution of the dust masses shown in the figure. The amount of dust destroyed by interstellar SN shocks depends on the age of the system: at the time corresponding to $z = 6.4$, we find that this effect reduces the mass of dust by 30% in both star formation models. On longer timescales, dust destruction is more pronounced in the case of a constant star formation rate (SN progenitors continue to form) resulting in more than 50% dust mass reduction at $z = 4.1$. Conversely, assuming the simulated star formation history, the fraction of dust destroyed at $z = 4.1$ is only 20%. This is due to SFR (and therefore SN rate) quenching by AGN-feedback and by the larger relative contribution of AGB stars in this model (see below).

As expected on the basis of the adopted stellar dust yields, the dominant dust component is found to be carbon dust, with silicates and other dust species being a factor 10 less abundant. Moreover, AGB stars are found to give a significant contribution to dust production at high redshift, accounting for $\sim 80\%$ of the total mass of dust at $z = 6.4$. In particular, AGB stars start to contribute to carbon dust production already 200 Myr after the onset of star formation, but their contribution remains sub-dominant until the last major burst of star formation, which occurs at $z = 8.5$ (0.6 Gyr). Following this burst, the mass of dust produced by AGB stars steeply rises for all the dust species. In fact, stars formed in this last major burst have nearly solar metallicities and their contribution to silicates and other dust components is no longer negligible.

These results depends on the adopted star formation history. When a constant star formation rate is assumed, as shown in the right panel of Fig. 6, the total mass of dust at $z = 6.42$ is a factor 2 smaller and the contribution of AGB stars is $\sim 50\%$. Since the stellar metallicities in this case are smaller, the contribution of AGB stars to silicate and other dust components are negligible.

We stress that, although the star formation history of the QSO host galaxies is still largely unknown, our analysis indicate that the contribution of AGB stars to dust production cannot be neglected,

even at the most extreme redshifts currently accessible to observations.

Additional constraints on the chemical evolution model can be obtained from observations of the metallicity and elemental abundances in the Broad Line Region (BLR) of the QSO. In fact, the detection of metal lines such as Fe (Barth et al. 2003), CII (Maiolino et al. 2005), and OI (in absorption, Becker et al. 2006) indicates that the ISM of the QSO host was significantly enriched by heavy elements. In a recent analysis, Juarez et al. (2009) investigated the metallicity of the BLR of a sample of 30 QSOs in the range $4 < z < 6.4$, including J1148+5251, using the (SiIV+OIV)/CIV ratio, which is a good metallicity tracer (Nagao et al. 2006). According to this analysis, the observed ratios do not show any correlation with redshift and correspond to metallicities which are several times solar.

In Fig. 7 we show the predicted evolution of the total metallicity in solar units (solid line) for the two star formation models shown in Fig. 6. The shaded area indicates the metallicity level inferred from observations of the narrow line regions (NLR) of a sample of high- z radio-galaxies, which shows no evolution over the redshift range $1 \leq z \leq 4$ (Matsuoka et al. 2009). Juarez et al. (2008) determined the metallicity of the BLR of J1148+5251. Since the BLR is a small nuclear region, of less than a few pc, containing a total mass of $\sim 10^4 M_{\odot}$, we consider this measurement to be an upper limit to the metallicity of the host galaxy. Conversely, the NLR has a size which is roughly comparable to the size of the host galaxy and represents a good tracer of the chemical properties on galactic scales (Matsuoka et al. 2009 and references therein).

Adopting the star formation history predicted by the simulation of Li et al. (2007, left panel), the ISM reaches the solar metallicity already at $z \sim 8$, and remains constant thereafter. A delayed metal-enrichment is found if a constant star formation rate is assumed (right panel) and the predicted metallicity at $z = 6.4$ is $\sim 0.4 Z_{\odot}$. Both models are consistent with the upper limit to the total metallicity derived from observational data for J1148+5251, and are in good agreement with the data inferred from NLRs observations at $z \sim 4$.

Finally, we would like to comment on the so-called "Carbon problem" pointed out by Juarez et al. (2009). These authors argue that the lack of evolution of the observed (SiIV+OIV)/CIV ratio between $4 \leq z \leq 6.4$ suggests that the abundance of carbon relative to silicon and oxygen also does not evolve significantly. If carbon is mostly produced by AGB stars, the bulk of its production must be delayed with respect to that of α -elements and we should expect to see an evolution at $z > 6$. However, the dotted lines in Fig. 7 show that both star formation models predict a (Si+O)/C ratio of ~ 6 at $z = 6.4$, with only a mild evolution at lower redshifts. The evolution is more pronounced in the left panel (a factor 2 over the redshift range $4.2 < z < 6.42$) because at $z \leq 6.4$ we expect to see the contribution to carbon (and carbon dust) enrichment of intermediate mass stars formed in the last major burst of star formation. As already discussed above, the contribution of intermediate mass stars is much less important when a constant star formation rate is assumed (right panel). The resulting mild evolution indicates that carbon production by massive short-lived stars, progenitors of SNe, is not negligible relative to that of longer-lived intermediate mass stars, at least according to the stellar metal yields adopted in the present paper.

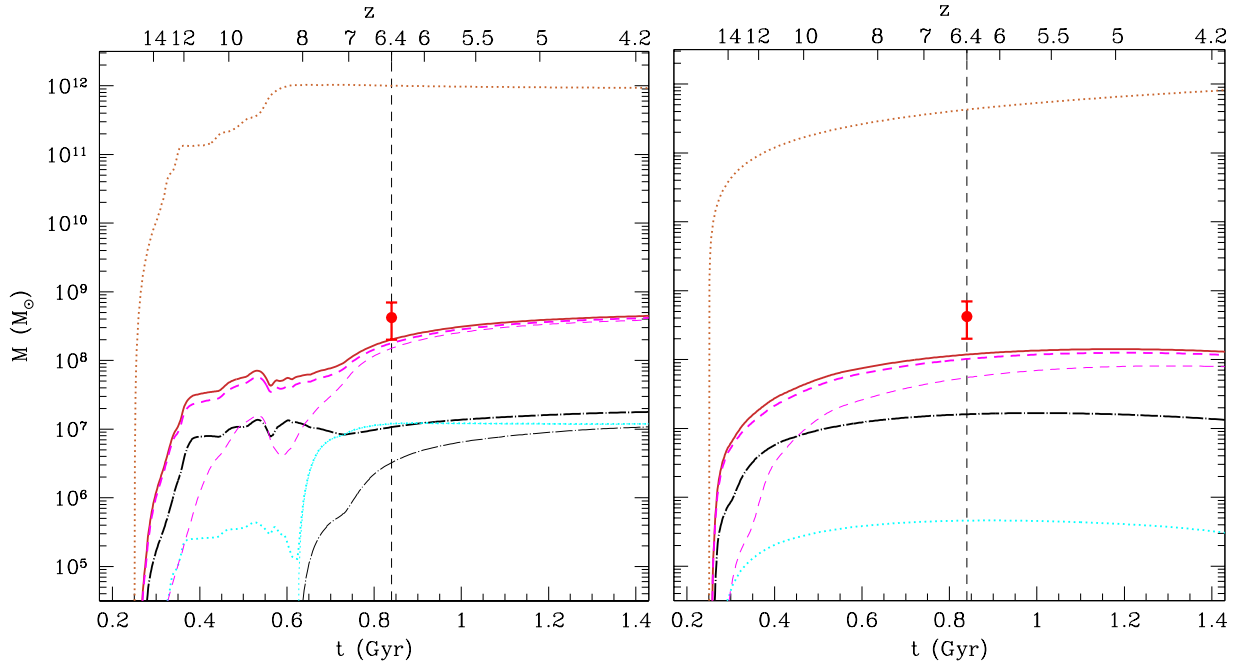


Figure 6. Chemical evolution of the high redshift quasar SDSS J1148+5251 corresponding to the star formation histories shown in Fig. 5 (left panel, SFR simulated by Li et al. (2007); right panel, constant SFR with the average value of $1000M_{\odot}\text{yr}^{-1}$). The lines represent the evolution of the mass of stars (dotted) and dust (solid); the lower dashed, dotted and dashed-dotted lines indicate the time evolution of the three main dust components, carbon, silicate and other dust grains, respectively. Thin lines represent the contribution of AGB stars only. The vertical dashed line indicates the Hubble time corresponding to $z = 6.4$ and the point with errorbars the assumed value for the observed dust mass (see text).

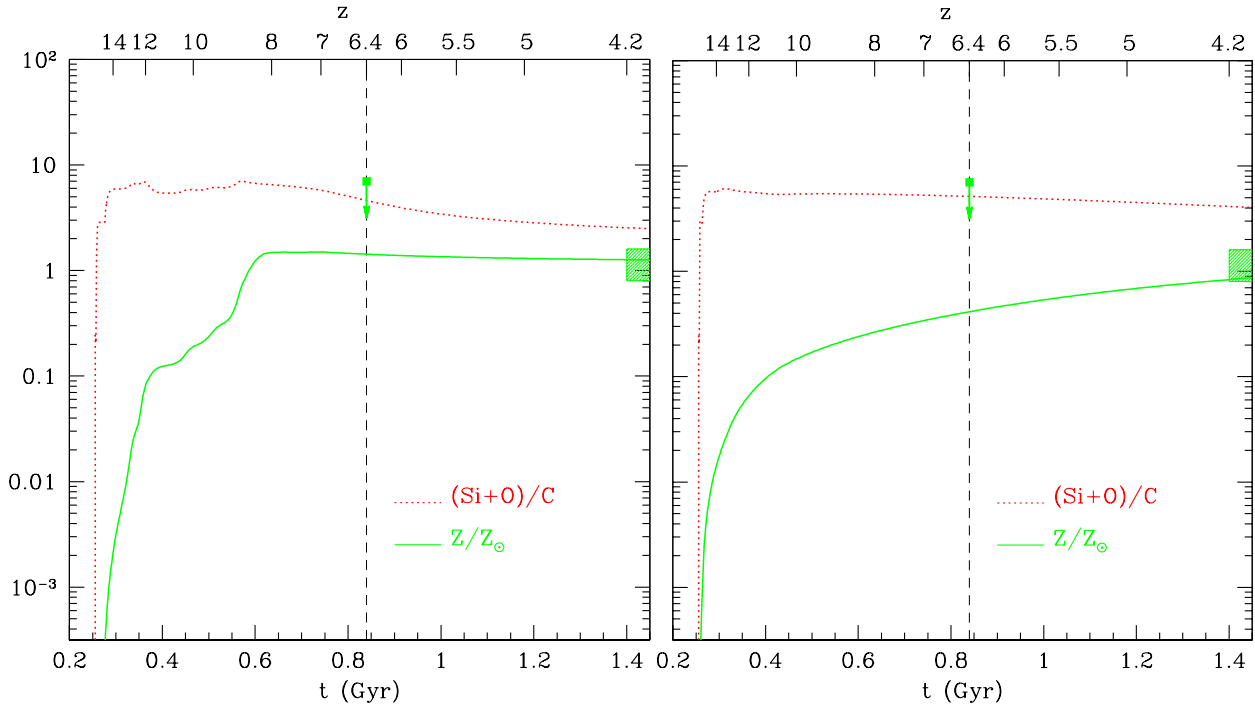


Figure 7. Chemical evolution of the high redshift quasar SDSS J1148+5251 corresponding to the star formation histories shown in Fig. 5 (left panel, SFR simulated by Li et al. (2007); right panel, constant SFR with the average value of $1000M_{\odot}\text{yr}^{-1}$). The solid line represent the evolution of the metallicity in solar units. The upper limit is derived from the metallicity measured in the BLR (Juarez et al. 2009) and the shaded area indicates the range of values derived from NLRs of a sample of lower- z radio-galaxies (Matsuoka et al. 2009). The dotted line represent the evolution of the (Si+O)/C elemental ratio. The vertical dashed line indicates the Hubble time corresponding to $z = 6.4$.

6 DISCUSSION AND CONCLUSIONS

In this work we show that the role of AGB stars in cosmic dust evolution at high redshift might have been over-looked. We develop a chemical evolution model which follows the evolution of metals and dust on the stellar characteristic lifetimes, taking into account dust destruction mechanisms. We use a grid of stellar dust yields as a function of the initial mass and metallicity over the range $1 - 40M_{\odot}$ and $0 - 1Z_{\odot}$. We adopt the stellar dust yields by Zhukovska et al. (2008) for AGB stars with stellar masses in the range $(1 - 7)M_{\odot}$ and the model of Bianchi & Schneider (2007) to account for dust production and destruction in the reverse shock of SNe, with progenitor stellar masses in the range $12 - 40M_{\odot}$.

Our results can be summarized as follows:

- A comparison of dust yields expected from AGB stars and SNe shows that carbon grains are the dominant dust component. Silicates and other dust components can only be produced by AGB stars with solar metallicities and by SNe when $Z \geq 10^{-2}Z_{\odot}$ but are always sub-dominant with respect to carbon grains. This is at odd with what has been generally adopted in chemical evolution models which, assuming a dust condensation efficiency of 1 for all refractory elements present in the ejecta, predict that SNe dominate silicate dust production and that AGB stars lead to a delayed injection of carbon dust (Dwek 1998; Dwek 2005; Galliano, Dwek & Chantal 2008).

- At early times, dust production is dominated by SNe as a consequence of the shorter lifetimes of their progenitor stars. AGB stars start to produce dust after about 30 Myr (i.e. when a $8M_{\odot}$ star evolves off the main sequence to the AGB phase). For our reference model, where we adopt a Larson IMF with $m_{ch} = 0.35M_{\odot}$ and stellar lifetimes from Raiteri et al. (1996), we find that the characteristic timescale at which AGB stars dominate dust production ranges between 150 and 500 Myr, depending both on the assumed star formation history and on the initial stellar metallicity. Hence, we conclude that these stellar dust sources must be taken into account at early cosmic epochs.

- This conclusion is only moderately dependent on the adopted stellar lifetimes, but it is significantly affected by variations of the IMF: for a $m_{ch} = 5M_{\odot}$, dust from AGB stars to dominate only on timescales larger than 1 Gyr, and SNe are found to dominate dust evolution when $m_{ch} \geq 10M_{\odot}$. Thus, variations of the stellar characteristic mass over cosmic history due to the smaller gas metallicity and/or to the larger cosmic microwave background temperature (see, e.g., Omukai et al. 2005) might significantly affect the origin and properties of dust in the high redshift Universe.

- We apply the chemical evolution model with dust to the host galaxy of the most distant QSO at $z = 6.4$, SDSS J1148+5251. Given the current uncertainties on the star formation history of the host galaxy, we have considered two models: (i) the star formation history obtained in a numerical simulation by Li et al. (2007) which predicts that a large stellar bulge is already formed at $z = 6.4$, in agreement with the local SMBH-stellar mass relation, through a series of strong bursts triggered by galaxy mergers in the hierarchical evolution of the system and (ii) a constant star formation rate of $1000M_{\odot}/\text{yr}$, as suggested by the observations if most of the FIR luminosity is due to young stars. In the latter case, the stellar mass at $z = 6.4$ is compatible with estimates of the dynamical mass derived by observations. The total mass of dust predicted at $z = 6.4$ by the first model is $2 \times 10^8 M_{\odot}$, within the range of values inferred by observations, with a substantial contribution ($\sim 80\%$) of AGB-dust. When a constant star formation rate is adopted, the contribution of AGB-dust decreases to $\sim 50\%$ but the total mass of dust formed

is a factor 2 smaller. Both models predict a rapid enrichment of the ISM with metals and a relatively mild evolution of the carbon abundance, in agreement with observational constraints.

The evolution of dust in the high-redshift Universe is still very uncertain. Some of the chemical evolution models with dust developed so far have been aimed at reproducing the elemental abundances of the gas and dust phases of the ISM of our galaxy (Dwek 1998; Falceta-Goncalves 2008; Zhukovska et al. 2008) and of local ellipticals and dwarf irregulars (Calura, Pipino & Matteucci 2008). In early galaxies, a crucial unknown is the relative contribution of SNe and AGB stars. It is generally found that there is no difficulty in producing highly dusty galaxies at $z \geq 5$ if SNe are an important contributor to interstellar dust. However, the models developed so far assume that all refractory elements present in SN ejecta form dust grains with a condensation efficiency of 1 (Dwek et al. 2007) or neglect dust destruction mechanisms (Morgan & Edmunds 2003).

The evolution of metals and dust in the host galaxy of the most distant quasar at $z = 6.4$ SDSS J1148+5251 has been also investigated by Dwek et al. (2007) which show that an average SN must condense a dust mass of $1M_{\odot}$ to reproduce the dust-to-gas ratio inferred from the observations (0.0067), when a gas mass of $3 \times 10^{10}M_{\odot}$ and a dust mass of $2 \times 10^8M_{\odot}$ are assumed. Since the observed dust yield is much lower (the largest observed dust yield is $\sim 0.054M_{\odot}$, Rho et al. 2008), the authors suggest that MC-grown dust or dust formed around the AGN (i.e. in outflows from the broad line regions, Elvis et al. 2002) must be taken into account. Our results suggest the alternative possibility that AGB stars might significantly contribute to dust production even at redshifts $z \geq 6$. For a comparison, we can infer from figure 8 in Dwek et al. (2007) that, in order to reproduce the dust-to-gas ratios predicted by our SFR models for SDSS J1148+5251 ($(1 - 6.7) \times 10^{-4}$ at $z = 6.4$), a dust yield per SN of about $0.1M_{\odot}$ would be required. This is larger than our adopted SN yields, the difference being compensated by the additional contribution to the dust budget provided by AGB stars.

More recently, Li et al. (2008) have applied a three-dimensional Monte Carlo radiative transfer code to the hydrodynamic simulations of Li et al. (2007) to model the dust properties of J1148+5251 and find that a supernova-origin dust model may be able to explain the observed dust properties. Yet, dust destruction in the ISM is not explicitly taken into account. Moreover, these models make the a-priori assumption that at redshift above 6, when the age of the Universe is less than 1 Gyr, the major alternative source of interstellar dust, namely AGB stars, have not yet evolved to their dust-production stage.

Our results show that stellar sources can account for the huge dust masses inferred from observations of distant QSOs. Although the star formation history of the QSO host galaxies is still largely unknown, our analysis indicate that the contribution of AGB stars to dust production cannot be neglected, even at the most extreme redshifts currently accessible to observations. Yet, since AGB winds are not efficient to disperse dust through the galaxy, SNe are still required to efficiently re-distribute dust on galactic scales (Jones 2005).

The nature and properties of the grains responsible for dust extinction in high-redshift QSOs and GRBs host galaxies (Maiolino et al. 2004; Stratta et al. 2007; Gallerani et al. in prep) are likely to depend more on the specific host galaxy star formation history than on redshift. Future observations aimed at constraining the properties of dust in high redshift QSOs might be a powerful probe of

star formation and QSO feedback regulating the BH-galaxy coevolution.

ACKNOWLEDGMENTS

We thank the anonymous referee for the careful reading and the insightful comments which helped us to improve the clarity of the paper. We are grateful to A. Ferrara, S. Gallerani, H. Gomez, A. Jones, R. Maiolino, D. Maoz, A. Marconi and S. Salvadori for useful suggestions. R. Schneider acknowledges the support and hospitality of the Dark Cosmology Center. The Dark Cosmology Centre is funded by the Danish National Research Foundation.

REFERENCES

- Barth A.J., Martini P., Nelson C.H., Ho L.C., 2003, *ApJ*, 594, L95
- Beelen A., Cox P., Benford D.J., Dowell C.D., Kovacs A., Bertoldi F., Omont A., Carilli C.L., 2006, *ApJ*, 642, 694
- Becker G.D., Sargent W.L.W., Rauch M., Simoncoe R.A., 2006, *ApJ*, 640, 69
- Bertoldi F. & Cox P. 2002, *A&A* 884,L11
- Bertoldi F., Carilli C.L., Cox P., Fan X., Strauss M.A., Beelen A., Omont A., Zylka R., 2003, *A&A*, 406, L55
- Bianchi S., Schneider R., 2007, *MNRAS*, 378, 973
- Calura F., Pipino A., Matteucci F., 2008, *A&A*, 479, 669
- Carilli C.L., Bertoldi F., Rupen M.P., Fan X., Strauss M.A., Menten K.M., Kreysa E., Schneider D.P., Bertarini A., Yun M.S., Zylka R., 2001, *ApJ* 555, 625
- Carilli C.L., Walter F., Bertoldi F., Menten K.M., Fan X., Lewis G.F., Strauss M.A., Cox P., Beelen A., Omont A., Mohan N., 2004, *AJ*, 128, 997
- Clayton D. D., Arnett D., Kane J. & Meyer B. S., 1997, *ApJ*, 486, 824
- Clayton D. D., Deneault E. A.-N., Meyer B. S., 2001, *ApJ*, 562, 480
- Draine B.T., 1990, in *The evolution of the interstellar medium*, ed. L. Blitz. (San Francisco ASP), ASP Conf. Proc., 12, 193
- Dunne L., Eales S., Ivison R., Morgan H., Edmunds M., 2003, *Nature*, 424, 285
- Dwek E., 1998, *ApJ*, 302, 363
- Dwek E., Galliano F., Jones A.P., 2007, *ApJ*, 662, 927
- Dwek E., 2005, in *The Spectral Energy Distributions of Gas-Rich Galaxies: Confronting Models with Data*, ed. C. Popescu & R.J. Tuffs. (Heidelberg, Germany) AIP Conf. Proc., 761, 103
- Elmhamdi A., Danziger I. J., Chugai N., Pastorello A., Turatto M., Cappellaro E. et al., 2003, *MNRAS*, 338, 939
- Elvis M., Marengo M., Karovska M., 2002, *ApJ*, 567, L107
- Falceta-Goncalves D., 2008, *A&A*, 478, 151
- Fan X., Strauss M.A., Schneider D.P., Becker R.H., White R.L. et al., 2003, *AJ*, 125, 1649
- Feder J., Russell K. C., Lothe J., Pound G. M., 1966, *Advances in Physics*, 15, 111
- Ferrarotti A.S., Gail H.P., 2006, *A&A*, 447, 553
- Freudling W., Corbin M.R., Korista K.T., 2003, *ApJ*, 587, L67
- Galliano F., Dwek E., Chaniai P., 2008, *ApJ*, 672, 214
- Hines D. C., Rieke G. H., Gordon K. D., Rho J., Misselt K. A., Woodward C. E. et al., 2004, *ApJS*, 154, 290
- Hopkins P. F., Strauss M. A., Hall P. B., Richards G. T., Cooper A. S., Schneider D. P. et al. 2004, *AJ*, 128, 1112
- Hughes D.H., Serjeant S., Dunlop J., Rowan-Robinson M., Blain A., Mann R.G., Ivison R., et al. 1998, *Nature*, 394, 241
- Jones A.P., Tielens A.G.G.M., Hollenbach D.J., McKee C.F., 1994, *ApJ*, 433, 797
- Jones A.P., Tielens A.G.G.M., Hollenbach D.J., 1996, *ApJ*, 469, 740
- Jones A.P., 2005, in *The Dusty and Molecular Universe: a prelude to Herschel and ALMA*, ed. by A. Wilson (Noordwijk ESA), ESA SP 577, 239
- Juarez Y., Maiolino R., Mujica R., 2008, *RMxAC*, 32, 105
- Juarez Y., Maiolino R., Mujica R., Pedani M., Marinoni S., Nagao T., Marconi A., Olive E., 2009, *A&A*, 494, 25
- Karakas A.I., Lattanzio J.C., 2003, *Publications of the Astronomical Society of Australia*, 20, 279
- Kemper F., de Koter A., Waters L.F.B.M., Bouwman J., Tielens A.G.G.M., 2002, *A&A*, 384, 585
- Kozasa T., Hasegawa H., Nomoto K., 1991, *A&A*, 249, 474
- Krause O., Birkmann S. M., Rieke G. H., Lemke D., Klaas U., Hines D. C., 2004, *Nature*, 432, 596
- Larson R.B., 1998, *MNRAS*, 301, 569
- Ledoux C., Bergeron J., Petitjean P., 2002, *A&A*, 385, 802
- Li Y., Hernquist L., Robertson B., Cox T.J., Hopkins P.F., Springel V., Gao L., Di Matteo T. et al., 2007, *ApJ*, 665, 187
- Li Y., Hopkins P.F., Hernquist L., Finkbeiner D.P., Cox T.J., Springel V., Jiang, L., Fan X., Yoshida N., 2008, *ApJ*, 678, 41
- Maiolino R., Comastri A., Gilli R., Nagar N. M., Bianchi S., Bker T., Colbert E., Krabbe A., Marconi, A., Matt, G., Salvati, M., 2003a *MNRAS*, 344, L59
- Maiolino R. Cox, P., Caselli P., Beelen A., Bertoldi F., Carilli C. L., et al. 2005, *A&A*, 440, L51
- Maiolino R., Juarez Y., Mujica R., Nagar N.M., Olive E., 2003b, *ApJ*, 596, L155
- Maiolino R., Nagao T., Marconi A., Schneider R., Bianchi S., Pedani M., Pipino A., Matteucci F., Cox P., Caselli P., 2006, *MmSAI*, 77, 643
- Maiolino R., Schneider R., Oliva E., Bianchi S., Ferrara A., Mannucci F., Pedani M., Roca Sogorb M., 2004, *Nature*, 431, 533
- Mannucci F., Della Valle M., Panagia N., 2006, *MNRAS*, 370, 773
- Maoz D. 2008, *MNRAS*, 384, 267
- Marchenko S. V., 2006, in Lamers H. J. G. L. M., Langer N., Nugis T., Annuk K., eds, ASP Conf. Ser. 353, 299
- Matsuoka K., Nagao T., Maiolino R., Marconi A., Taniguchi Y., 2009, submitted to *A&A*
- Meikle W., Mattila S., Pastorello A., Gerardy C., Kotak R., Sollerman J. et al. 2007, *ApJ*, 665, 608
- Morgan H.L., Edmunds M.G., 2003, *MNRAS*, 343, 427
- Nagao T., Marconi A., Maiolino R., 2006 *A&A*, 447, 157
- Nozawa T., Kozasa T., Umeda H., Maeda K., Nomoto K., 2003, *ApJ*, 598, 785
- Nozawa T., Kozasa T., Habe A., Dwek E., Umeda H., Tominaga N., Maeda K., Nomoto K. 2007, *ApJ*, 666, 955
- Omont A., Cox P., Bertoldi F., McMahon R.G. et al. 2001, *A&A* 374, 371
- Omukai K., Tsuribe T., Schneider R., Ferrara A., 2005, *ApJ*, 626, 627
- Padovani P., Matteucci F., 1993, *ApJ*, 416, 26
- Pentericci L., Fan X., Rix H.W., Strauss M.A., Narayanan V.K., Richards G.T., Schneider D.P., Krolik J., Heckman T., et al. 2002, *AJ*, 123, 2151
- Pettini M., Smith L.J., Hunstead R.W., King D.L., 1994, *ApJ*, 426, 79
- Prochaska J.X., Wolfe A.M., 2002, *ApJ*, 566, 68
- Raiteri C.M., Villata M., Navarro J.F., 1996, *A&A*, 315, 105
- Rho J., Kozasa T., Reach W. T., Smith J. D., Rudnick L., DeLaney T., Ennis J. A., & Gomez H., 2008, *ApJ*, 673, 271
- Rho J. et al. 2009, conference proceeding for "Cosmic Dust - Near and Far" (Heidelberg, Germany), eprint arXiv:0901.1699
- Robson I., Priddey R.S., Isaak K.G., McMahon R.G., 2004, *MNRAS*, 351, L29
- Salpeter E.E., 1974, *ApJ*, 193, 579
- Salvadori S., Ferrara A., Schneider R. 2008, *MNRAS*, 386, 348
- Schneider R., Ferrara A., Salvaterra R. 2004, *MNRAS*, 351, 1379
- Smail I., Ivison R.J., Blain A.W., 1997, *ApJ*, 490, L5
- Smart S. J., Eldridge J. J., Crockett R. M., Maund J. R., 2009, *MNRAS*, submitted, eprint arXiv:0809.0403
- Stratta G., Maiolino R., Fiore F., D'Elia V., 2007, *ApJ*, 661, L9
- Sugerman B. E. K., Ercolano B., Barlow M. J., Tielens A. G., Clayton G. C., Zijlstra A. A. et al. 2006, *Science*, 313, 196
- Tielens A.G.G.M., 1998, *ApJ*, 499, 267
- Todini P., Ferrara A., 2001, *MNRAS*, 325, 726
- van den Hoek L.B., Groenewegen M.A.T., 1997, *A&AS*, 123, 305
- Walter F., Carilli, C., Bertoldi, F., Menten, K., Cox, P., Lo, K.Y., Fan, X., Strauss, M.A., 2004, *ApJ*, 615, L17

- Wilson T., Batrla W. 2005, *A&A*, 430, 561
Willott C.J., McLure R.J., Jarvis M.J., 2003, *ApJ*, 587, L15
Whittet D.C.B 1992, in *Dust in the Galactic Environment*, IOP Publishing
Bristol
Woosley S.E., Weaver T.A., 1995, *ApJ*, 101, 181
Wooden D. H., Rank D. M., Bregman J. D., Witteborn F. C., Tielens A. G.,
Cohen M. et al 1993, *ApJS*, 88, 477
Zhukovska S., Gail H.P., Tieloff M., 2008, *A&A*, 479, 453